



# Comparison of machine learning algorithms and feature extraction techniques for the automatic detection of surface EMG activation timing

Valentina Mejía Gallón<sup>\*</sup>, Stirley Madrid Vélez, Juan Ramírez, Freddy Bolaños

*Department of Mechanical Engineering, Universidad Nacional de Colombia, Medellín 050034, Colombia*



## ARTICLE INFO

### Keywords:

Electromyography (EMG)  
Deep learning  
Classification  
Discrete wavelet transform (DWT)

## ABSTRACT

This paper presents a methodology for automatically detecting muscular activity by denoising, extracting features, and classifying surface electromyography (sEMG) signals. The proposed methodology utilizes the Discrete Wavelet Transform (DWT) and Willison's Amplitude Algorithm (WAMP) for feature extraction. Five classification methods, including Neural Networks (NN), Classification Vector, XGBoost, Light Gradient Boosting Machine (LGBM), and ExtraTree, were evaluated using F-Measure, Precision, and Recall as performance metrics. Through k-fold cross-validation, the XGBoost algorithm, when combined with the Eigen values feature, achieved the highest training performance with an F1-Score of 98.71 %. For the test group, the LGBM classifier using WAMP, and NN with both WAMP and Eigen values as features, demonstrated the best average performance with F1-Scores of  $96.52 \pm 3.45\%$  and  $96.52 \pm 3.07\%$ , respectively. These results highlight the precision and performance of the proposed approach in detecting EMG signals. Moreover, the framework has the potential to support clinicians in diagnosing neuromuscular disorders and developing human-machine interfaces.

## 1. Introduction

One of the significant challenges in surface electromyography (sEMG) applications is accurately identifying the onset and offset of muscle activation. The development of electromyography-powered assistive devices, clinical analysis, and muscle-machine interface applications heavily relies on the timing of muscle recruitment. However, traditional methods for identifying muscle activation involve visual inspections by trained experts, which are time-consuming, not reproducible, and impractical for large databases. Additionally, these methods are prone to human errors. Semi-automated techniques often involve setting a detection threshold and using a signal envelope obtained from temporal, spectral, or energy (TKEO) analysis [1–3]. Despite being semi-automated, these techniques still require manual input to determine optimal detection algorithm parameters and need adjustment for each muscle group, individual, and movement. Consequently, they are inefficient when dealing with large amounts of data [4]. Moreover, due to the stochastic nature of sEMG, the uncertainty in detecting muscle activation and deactivation increases during rapid muscle contractions, and there can be considerable variation in signal-to-noise ratios (SNR) between different muscle groups. Machine learning has demonstrated effectiveness in interpreting, classifying, and detecting sEMG signals

[1,4–10]. Various studies have focused on gesture classification, muscle fatigue detection, and unsupervised learning for classifying neuromuscular disorders [11–13]. Support Vector Machines (SVM) [14,15] and Convolutional Neural Networks [11,12,16] are among the most commonly used models. SVM performs well with limited training data, while Convolutional Neural Networks excel at learning and modeling complex non-linear relationships. Less explored is the field of muscle activation, which poses multiple challenges such as proper processing of electromyography signals, feature selection, and identifying the best model for classifying the neutral and activated states of different muscle groups. For instance, Di Nardo developed a high-throughput approach (DEMANN) that employed the wavelet spectrogram of sEMG signals as input to a convolutional neural network [4]. The method achieved prediction accuracies exceeding 90 % for muscle activation, even with high signal variability. Similarly, Ghislieri trained a Long Short-Term Memory (LSTM) neural network, which outperformed semi-automated methods such as TKEO and Stat, even at medium and low noise ratios [17]. Therefore, there is a need for further research proposing automated learning methods for muscle activation detection [4,17–19]. The objective of this study is to determine the optimal combination of learning methods and features for the electromyography signal, based on performance and accuracy in detecting muscle activation and

\* Corresponding author.

E-mail address: [vamejag@unal.edu.co](mailto:vamejag@unal.edu.co) (V.M. Gallón).

deactivation, regardless of the individual, muscle group, or performed movement. The paper is organized as follows: [Section 2](#) describes the implemented methods and materials, including data acquisition, signal preprocessing, feature extraction, and classification models (see [Fig. 1](#)). [Section 3](#) presents the complete experimental results, including various measures of classification precision. In [Section 4](#), the performance of different models in detecting false positives and dynamic muscle activations is analyzed and compared. Finally, the conclusions are provided in [Section 5](#).

## 2. Materials and methods

[Fig. 1](#) illustrates the options available at each stage of a generic EMG detection system. To identify the optimal combination of learning methods and characteristics for the electromyography signal, characteristics based on both wavelet decomposition and Willison's signal-by-amplitude temporal analysis were utilized and tested.

The first step involved obtaining the sEMG training and test sets and extracting the corresponding features. The training set comprised 10 records, incorporating different movements proposed in the test set, along with the muscles specified in the study (Biceps Brachii, brachioradialis, vastus medialis). Additionally, different tests with other muscles were included (Triceps, vastus lateralis) to introduce variability to the test and prevent bias during validation with the test group. Ultimately, the training group was performed by the participants involving predefined movements for the study. The test group comprised 12 records, assigning three records to each of the four participants, corresponding to the three defined muscles. This approach aimed to ensure diversity in the test set and avoid potential biases in the validation process with the test group. Subsequently, the individual and joint evaluation of these characteristic groups was performed using five different classification methods. Finally, the models with various combinations of characteristics were evaluated and compared across different muscle groups and individuals using three evaluation metrics: F1 Score, Precision, and Recall.

To assess the results obtained for each model, the Friedman post-hoc test methodology proposed by [20] was employed to compare multiple algorithms on multiple data sets. The null hypothesis of the Friedman test assumes no statistical difference in the mean values of F1 Score, Precision, and Recall for the 15 tested models. Rejecting this null hypothesis indicates that one or more pairs of classifiers perform differently. The methodology uses the metrics obtained from each test in the experimental setup, which involves executing three movements for four subjects, resulting in a total of 12 records or data groups. The Friedman test categorizes the data from each classifier and resampling method, analyzing the rank values. If the null hypothesis is rejected, a post-hoc test, such as the Nemenyi test [21], is conducted to determine which means differ.

### 2.1. Data acquisition

The proposed setup utilized the APISI platform (Hardware + Software), developed by the GIBIR research group of the National University of Colombia, as depicted in [Fig. 2](#). The APISI device underwent validation by comparing it with the commercial DataLITE Wireless EMG Sensor from Biometrics Ltd. The root mean square (RMS) difference between the signals was found to be  $0.051 \pm 0.001$  mV.

The APISI platform allows for the recording of electromyography signals using surface bipolar Ag/AgCl electrodes, with a maximum of two sEMG channels. To ensure maximum information retrieval while adhering to Nyquist's theorem, a sampling frequency of 5000 Hz was set, as the sEMG frequency spectrum typically lies between 0 and 500 Hz [22]. Subsequently, the acquired signal was filtered using an analog Butterworth bandpass filter (5–500 Hz) and a 60 Hz Notch filter to mitigate noise originating from the electrical network. [Table 1](#) provides detailed information on the main characteristics of the device.

The experiments involved four individuals (subjects) without disabilities, with an average age of  $24 \pm 3$  years, including one male and three females. The experiments were conducted with the subjects using their dominant hand. Two subjects (male and female) were right-handed, while the other two subjects were left-handed. [Fig. 3.a, b](#) illustrates the electrode placement for each movement, which was validated by an expert and replicated for each subject. The experimental procedures, protocols, and informed consent were approved by the Ethical Committee of the Universidad Nacional de Colombia and conducted in accordance with the principles outlined in the Helsinki Declaration.

The test group consisted of subjects who were instructed to perform three specific movements, alternating between the rest and activation states. The movements and electrode placements were as follows:

- Concentric contraction of the short head of the Biceps Brachii (BB) muscle in the subject's dominant arm. The contraction was isotonic, unloaded, and involved an angular range of motion of the elbow from  $0^\circ$  to  $90^\circ$ . Bipolar electrodes were positioned on the muscle belly of the short head of the BB muscle, with a 20 mm spacing between the electrodes. The reference electrode was placed on the bony prominence of the elbow.
- Isometric contraction of the brachioradialis (BR) muscle during a supinated hand grip. The bipolar electrodes were positioned on the muscle belly of the BR muscle, and the reference electrode was placed at the same point as the BB muscle.
- Eccentric and concentric contraction of the vastus medialis oblique (VM) muscle during the execution of squats without weights, with a knee rotation angle ranging from  $0^\circ$  to  $45\text{--}60^\circ$ . Bipolar electrodes were placed along the thigh, with the proximal electrode located 50 mm above the upper border of the patella on the medial side, and the distal electrode located 20 mm from the

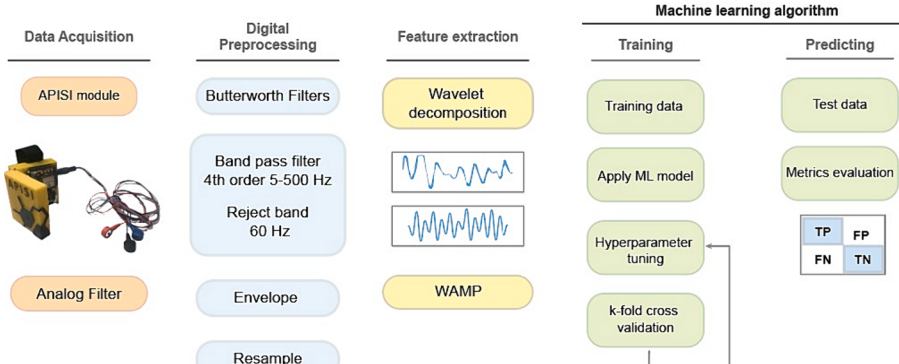


**Fig. 1.** Stages for muscle activation detection analysis, comprised of acquisition, preprocessing, feature extraction, and machine learning model.

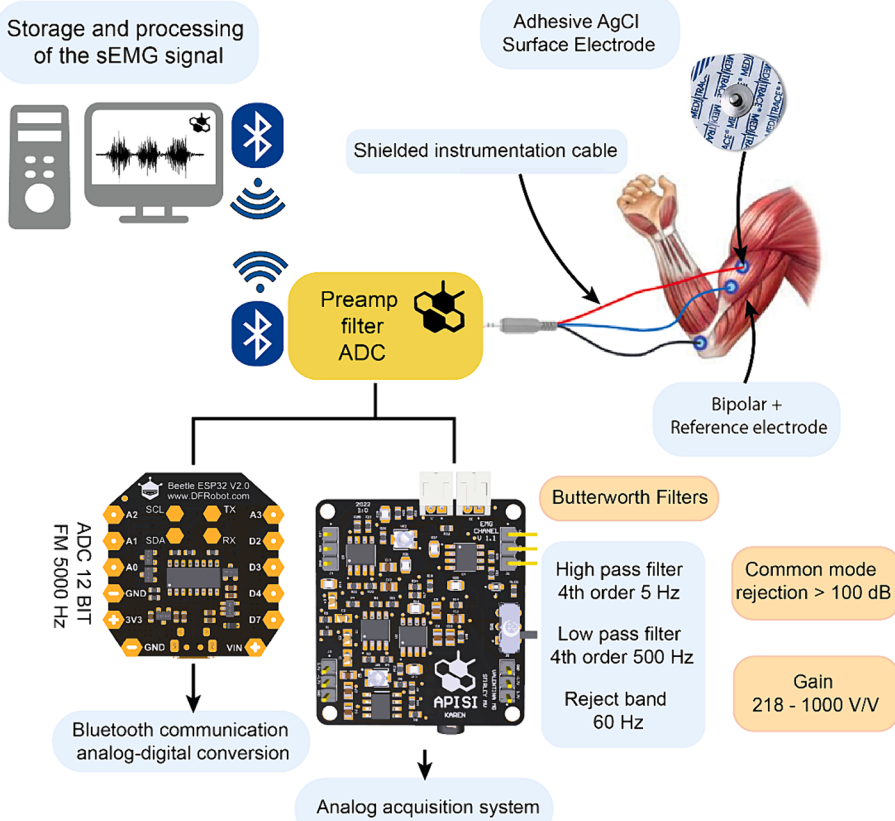


**Fig. 2.** APISI device and schematic of the assembly.

**Table 1**  
APISI sEMG module technical specifications.

| Item                   | Value                        | Description           |
|------------------------|------------------------------|-----------------------|
| Power supply           | 3.7 V, -3.7 V<br>Dual supply | 2 LiPo batteries      |
| Microcontroller        | -                            | ESP32-Beetle          |
| Communication Protocol | Bluetooth                    | Classic               |
| ADC conversor          | 12                           | bits                  |
| Resolution             | 0.91                         | mV                    |
| Sample frequency       | 5000                         | Hz                    |
| Channels               | 2                            | sEMG                  |
| Adjustable gain range  | 218–1000                     | V/V                   |
| Low-pass filter        | F <sub>c</sub> = 500 Hz      | 4th Orden Butterworth |
| High-pass filter       | F <sub>c</sub> = 5 Hz        | 4th Orden Butterworth |
| Band reject filter     | F <sub>r</sub> = 60 Hz       | 2nd Orden Notch       |
| Offset range           | 0–1.6                        | V                     |
| CMR                    | >100                         | dB                    |
| Card dimensions        | 37.7 × 41                    | mm                    |

proximal electrode in the same direction, on the belly of the VM muscle. The reference electrode was placed in the lower area of the patella.

The APISI device was connected to the signal software via Bluetooth, enabling the recording, visualization, and preprocessing of the signal. To validate the labeling of the acquired data for the development of supervised learning models, each movement was recorded on camera and synchronized with the data collection in the software. Furthermore, the labeling was verified by an sEMG expert. For each gesture, three seconds of the resting state were recorded at the beginning of each test, followed by three repetitions of the gesture execution. Fig. 3.c illustrates the recorded signal in the time domain for the three movements performed by subject 1.

## 2.2. Signal preprocessing

To ensure accurate signal analysis, the raw sEMG signal needs to be filtered due to potential disturbances from motion artifacts, power line interference, and other sources of noise [1,23]. In certain applications, rectification and normalization of the signal are also common for improved analysis results.

After recording the sEMG signal, the DC component was eliminated by shifting the baseline to 0 mV, resulting in a signal with both positive and negative values. Next, digital filters were applied, including a 5–500 Hz bandpass filter and a 60 Hz Notch filter. The signal was then scaled to a range between –1 mV and 1 mV.

Additionally, working with only positive values is often recommended. Therefore, a full wave rectification was performed to preserve the original information while ensuring positivity in the signal. Various methods can be used to smooth the rectified signal, reduce noise, and enhance true muscle activity. However, the performance of these methods may be affected by the signal-to-noise ratio (SNR), particularly as the dynamic nature of the signal causes the SNR to vary throughout the recording [24]. As strategy to assess classifiers and envelope features under SNR dynamics, an experimental sEMG dataset with varying levels of noise was created.

To simulate experimental surface EMGs with different noise levels, independently generated zero-mean white Gaussian noise was added to the filtered EMG signals. Fig. 4 illustrates the processed signal for subject 1. Each trial was assigned a specific SNR, and it is evident that lower SNRs significantly impede the visual identification of muscle activations. However, for the VM muscle, an SNR of 37 notably improves signal quality, facilitating accurate identifications.

To achieve different SNRs in the simulated surface EMG signals, ranging from 3 to 37, the standard deviation of the added noise was determined based on the natural SNR of the signal. The noise level was

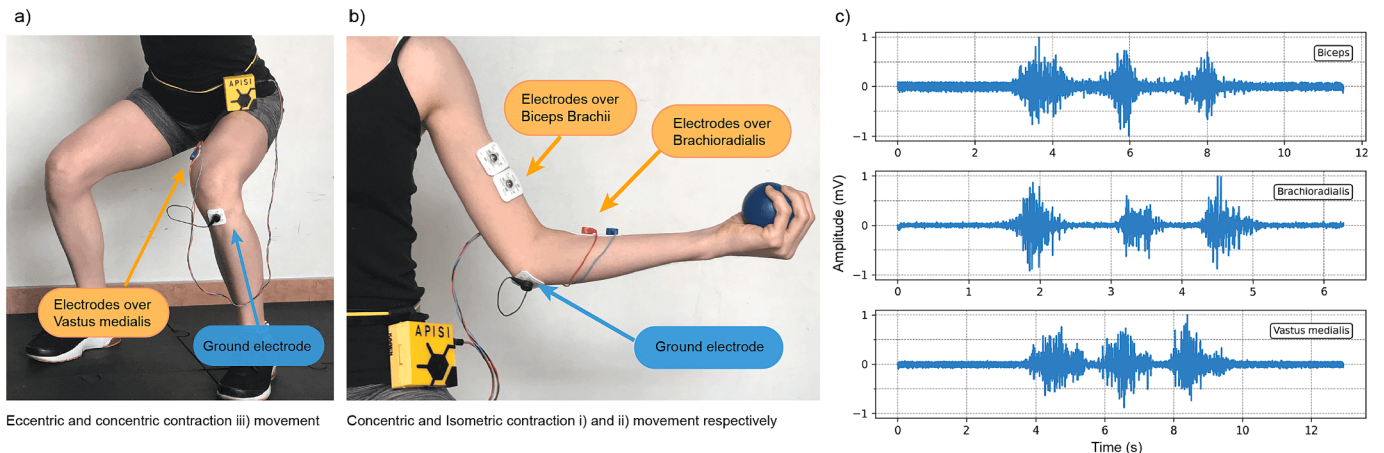


**Fig. 3.** (a) Electrodes position for iii) movement, Eccentric and concentric contraction of the vastus medialis. (b) Electrodes position for i) and ii) movement for the Biceps and brachioradialis. (c) Time domain sEMG signal per each movement from the group test subject 1.

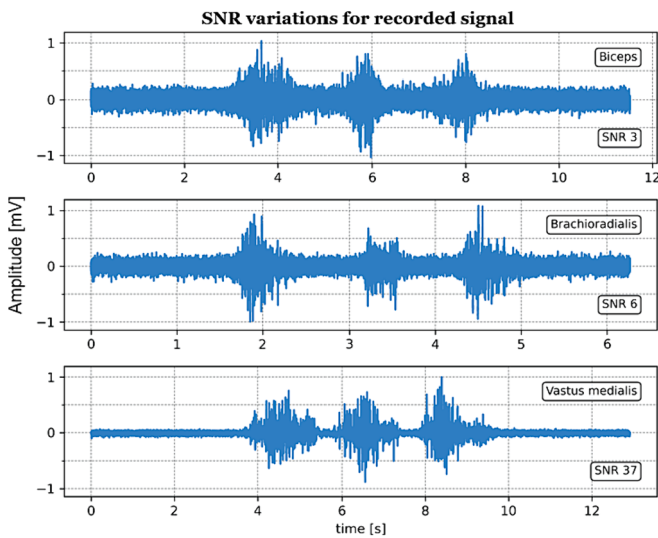


**Fig. 4.** Processed sEMG signals for Subject 1 in the Biceps (SNR 3), Brachioradialis (SNR 6), and VM (Original SNR of 37).

adjusted to correspond to the desired SNRs, taking into account that the natural SNR varied between 27 and 37 across samples. The selection of SNRs for each trial and participant was randomized, and the assigned SNRs are summarized in Table 2.

To reduce computational effort, it is preferable to work with data that retains the most relevant information from the original signal while having a small dimension. Among the techniques commonly used, the ones that focus on capturing the main characteristics of the EMG signal can be categorized into three types: time domain, frequency domain, and a combination of both [25–27]. However, due to the computational complexity associated with the combination of time and frequency domains, research and applications often employ the first two categories.

**Table 2**  
Assigned SNRs for Simulated EMG Signals.

| Movement |  | i) | ii) | iii) |
|----------|--|----|-----|------|
| Subject  |  |    |     |      |
| 1        |  | 3  | 6   | 37   |
| 2        |  | 10 | 3   | 27   |
| 3        |  | 16 | 6   | 30   |
| 4        |  | 20 | 10  | 27   |

For this study, the RMS envelope was implemented using a rolling window of 150 ms. RMS is a function of the signal amplitude and has been shown to be suitable for constant force and non-fatiguing contractions, effectively preserving important information from the original signal [26].

$$RMS = \sqrt{\frac{1}{N} \sum_{n=1}^N x(n)^2} \quad (1)$$

### 2.3. Feature extraction

One of the objectives of this study is to determine the optimal set of features that yields the best classification performance (F1-Score, Precision, and Recall) for the dataset. Identifying the best feature set can lead to improved classification performance and reduce the time required for feature extraction and classification.

Fig. 5 illustrates the process starting from the RMS envelope, as mentioned earlier. From each window of the RMS envelope signal, six features were extracted: five eigenvalues and one WAMP value. The window size was set to 200 ms with a 50 % overlap.

The maximum allowable number of eigenvalues is constrained by the upper limit of the window size. After experimenting with different eigenvalue quantities, five eigenvalues resulted in optimal results. Furthermore, Fig. 5(b) reveals that the initial eigenvalues effectively represent the predominant variance in the dataset. Retaining these primary principal components ensures the capture of the most relevant information in the dataset.

### 2.4. WAMP - Willison amplitude

Willison's Amplitude (WAMP) is a feature that reflects the activation of motor unit action potentials (MUAPs) and the level of muscle contraction [28]. It quantifies the number of times the amplitude of the EMG signal exceeds a predefined threshold within a time window.

$$WAMP = \sum_{n=1}^{N-1} f(|x(n) - x(n+1)|), \quad (2)$$

$$f(x) = \begin{cases} 1, & \text{if } x \geq \text{threshold} \\ 0, & \text{otherwise} \end{cases}, \quad (3)$$

where  $x(n)$  represents each of the signal samples out of a total of N samples in the sEMG register. To ensure comparability across conditions, a sliding window approach was adopted for all feature calculations, with a width of 200 ms and a 50 % overlap. Different thresholds were tested, depending on the noise levels in the resting state of each participant. Ultimately, the best results were obtained using the

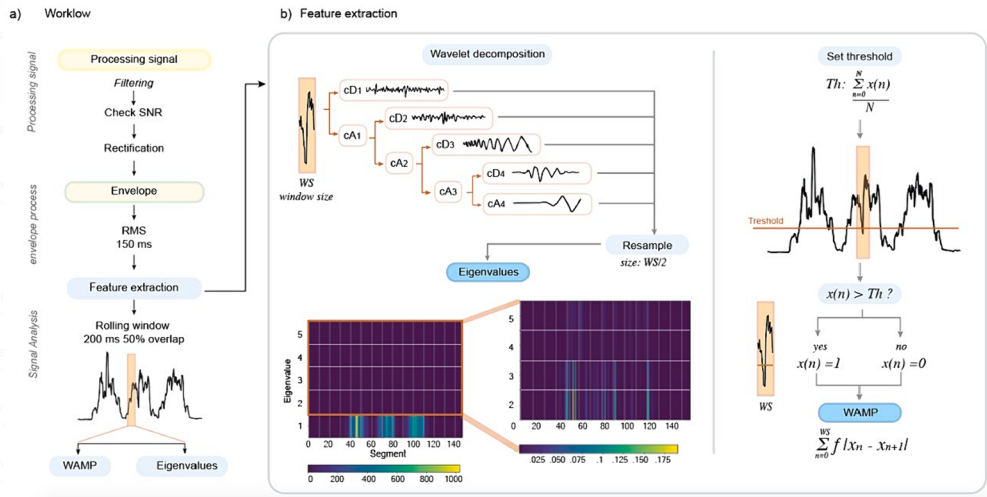


**Fig. 5.** (a) Workflow from data filtering to sEMG feature extraction. (b) Wavelet decomposition for the extraction of the eigenvalues and the algorithm used to calculate the Willison amplitude method.

threshold as the mean average of all recorded signals. Fig. 6 displays the RMS envelope of the contraction of the VM muscle. It demonstrates the relationship between the WAMP characteristic and the eigenvalues, which correspond to the original envelope of the sEMG signal.

## 2.5. WCM - wavelet correlation modes

The Wavelet Correlation Modes are eigenvalues that provide a concise representation of the information contained in the components of the Discrete Wavelet Transform. The signal  $x(t)$  is decomposed into approximation coefficients  $a(t)$  and detail coefficients  $d(t)$  at different levels, based on the desired level of signal division [29].

$$a_{j,k} = \int x(t)\phi_{j,k}(t)dt \quad (4)$$

$$d_{j,k} = \int x(t)\psi_{j,k}(t)dt \quad (5)$$

$\phi$  and  $\psi$  correspond to the father and mother wavelets, respectively.  $j$  and  $k$  are the scale and translation parameters. In this case, the smooth or low-frequency components of the signal are approximated using the father wavelet, while the detailed high-frequency components are represented by the mother wavelet. As a result, the discrete signal  $x(t)$  can be expressed in an orthogonal wavelet basis as follows:

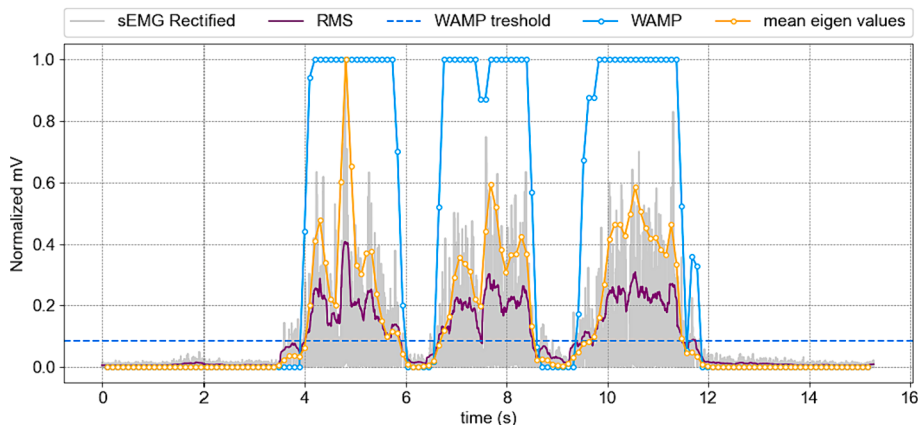


**Fig. 6.** Recorded signal of VM contraction for the test group with SNR of 37. For each recording window of 200 ms, the average of the five eigenvalues and the scaled WAMP value are plotted between (0.1) for the RMS envelope.

on the diagonal. Thus, the matrix can be decomposed as follows [33]:

$$x_{n \times p} = U_{n \times n} S_{n \times p} V_{p \times p}^T \quad (7)$$

The Python PyWavelets library was utilized for the implementation of the DWT. In this study, the father and mother wavelet were fixed and set to the same type, specifically Symlet of order 5. The decomposition level was set to 3, although exploring different levels of decomposition and wavelet families is a potential avenue for future research. The wavelet decomposition was performed up to four levels. To ensure consistent dimensions across different levels, each level of detail and approximation coefficients were resampled to match the dimensions of the first level. This resulted in a rectangular matrix with dimensions of  $5 \times \frac{b}{2}$ , where b represents the number of windows sampled in the signal. Fig. 5.b illustrates how three muscle activation pulses from the VM contraction exhibit a direct relationship with the eigenvalues. Notably, the first eigenvalue consistently has the highest magnitude across all samples within a range of 600–1000, while the remaining eigenvalues exhibit activation ranges between 0.075 and 0.175.

## 2.6. Classification models

The five selected classification algorithms for this study were Neural Networks (NN), Support Vector Machine (SVM), Extreme Gradient Boosting (XGB), Light Gradient Boosting Machine (LGBM), and Extremely Randomized Trees Classifier (ExtraTree) [34,35]. Machine learning algorithms have been widely applied in various fields and applications. However, when utilizing machine learning models, several important considerations need to be taken into account, including cross-validation, hyperparameter tuning, evaluation metrics, training data balance [36]. Hyperparameters are adjustable parameters that control the training process of a machine learning model. Selecting the optimal hyperparameter settings greatly impacts the performance of the model [36]. This often requires a comprehensive understanding of machine learning algorithms and the use of proper hyperparameter optimization techniques. In this study, the scikit-learn library was employed, which provides convenient tools such as GridSearchCV and RandomSearchCV estimators for hyperparameter tuning. Exhaustive hyperparameter tuning was performed for each model, with evaluation metrics including F1-Score, Precision, and Recall. Furthermore, the k-fold cross-validation technique was employed for model validation, utilizing 5-fold cross-validation. Cross-validation is a widely used technique in machine learning algorithms, as it enables the estimation of models with low bias. Table 3 presents the results, with the highest score per row indicated by bold cells.

The search for hyperparameters was conducted for each machine learning algorithm according to the input features. Therefore, out of three possible combinations of features (WAMP, eigenvalues, and the combination of both denoted as MIX) and five machine learning algorithms, 15 optimized models were obtained. Table 4 presents the best hyperparameters obtained for the tuning of each model.

**Table 3**  
Mean classification score on the training data set associated with different features.

| Algorithm          | NN                     | SVM                    | ExtraTree              | XGB                    | LGBM                   |
|--------------------|------------------------|------------------------|------------------------|------------------------|------------------------|
| Evaluation Metrics | <b>MIX</b>             |                        |                        |                        |                        |
| Accuracy           | <b>0.9473 ± 0.0219</b> | <b>0.9473 ± 0.0294</b> | <b>0.9294 ± 0.0233</b> | <b>0.9313 ± 0.0250</b> | <b>0.9510 ± 0.0232</b> |
| F1                 | <b>0.9516 ± 0.0200</b> | <b>0.9527 ± 0.0251</b> | <b>0.9367 ± 0.0193</b> | <b>0.9378 ± 0.0208</b> | <b>0.9554 ± 0.0209</b> |
| ROC AUC            | <b>0.9750 ± 0.0161</b> | <b>0.9619 ± 0.0264</b> | <b>0.9829 ± 0.0118</b> | <b>0.9864 ± 0.0087</b> | <b>0.9603 ± 0.0227</b> |
| <b>WAMP</b>        |                        |                        |                        |                        |                        |
| Accuracy           | <b>0.9520 ± 0.0248</b> | <b>0.9247 ± 0.0252</b> | <b>0.9294 ± 0.0233</b> | <b>0.9350 ± 0.0246</b> | <b>0.9510 ± 0.0232</b> |
| F1                 | <b>0.9562 ± 0.0225</b> | <b>0.9296 ± 0.0233</b> | <b>0.9367 ± 0.0193</b> | <b>0.9410 ± 0.0213</b> | <b>0.9554 ± 0.0209</b> |
| ROC AUC            | <b>0.9757 ± 0.0153</b> | <b>0.9154 ± 0.0330</b> | <b>0.9829 ± 0.0118</b> | <b>0.9844 ± 0.0133</b> | <b>0.9638 ± 0.0195</b> |
| <b>EIGEN</b>       |                        |                        |                        |                        |                        |
| Accuracy           | <b>0.9266 ± 0.0218</b> | <b>0.9463 ± 0.0266</b> | <b>0.9294 ± 0.0233</b> | <b>0.9350 ± 0.0352</b> | <b>0.9510 ± 0.0232</b> |
| F1                 | <b>0.9332 ± 0.0181</b> | <b>0.9517 ± 0.0231</b> | <b>0.9367 ± 0.0193</b> | <b>0.9415 ± 0.0297</b> | <b>0.9554 ± 0.0209</b> |
| ROC AUC            | <b>0.9855 ± 0.0113</b> | <b>0.9696 ± 0.0214</b> | <b>0.9829 ± 0.0118</b> | <b>0.9871 ± 0.0116</b> | <b>0.9676 ± 0.0220</b> |

**Table 4**

Summary for the best hyperparameter tuning results of the machine learning models.

| Algorithm   | MIX feature  | WAMP feature  | Eigen feature   |
|-------------|--|---|---|
| XGB         | Maximum tree's depth: 6<br>Learning rate: 0.01<br>Columns per tree: 0.9  | Maximum tree's depth: 3<br>Learning rate: 0.001<br>Columns per tree: 0.6  | Maximum tree's depth: 6<br>Learning rate: 1<br>Columns per tree: 0.8  |
| Extra Trees | Criterion: Gini<br>Max depth: 13<br>Estimators: 10   | Criterion: Gini<br>Max depth: 13<br>Estimators: 89  | Criterion: Gini<br>Max depth: 13<br>Estimators: 100   |
| LGBM        | Columns by per: 80 %<br>Gamma: 0.4<br>Maximum tree's depth: 18<br>L1 regularization: 100<br>L2 regularization: 1 | Columns by per: 30 %<br>Gamma: 0.3<br>Maximum tree's depth: 6<br>L1 regularization: 1e-5<br>L2 regularization: 10 | Columns by per: 60 %<br>Gamma: 0.3<br>Maximum tree's depth: 9<br>L1 regularization: 100<br>L2 regularization: 100 |
| SVM         | Regularization: 0.1<br>Gamma: 0.001  | Regularization: 100<br>Gamma: 0.001   | Regularization: 1<br>Gamma: 0.01  |
| NN          | Activation function: "tanh"<br>Alpha: 0.24Hidden layer size: (8,)  | Activation function: "logistic"<br>Alpha: 0.08Hidden layer size: (5,)   | Activation function: "tanh"<br>Alpha: 0.36Hidden layer size: (8,)   |

Each of the 15 models was trained using a training set consisting of 10 different recordings. These recordings involved participants performing muscle contractions and extensions of the Biceps, VM, Quadriceps, Brachioradialis, and Triceps. In total, 1040 samples or windows were recorded and labeled, with 0 representing no muscular activity and 1 representing muscle activity. The distribution of samples was approximately 40 % activation and 60 % deactivation. It is important to note that there was no distinction between individuals, muscles, or specific records in the labeling of the samples. The aim was for the model to learn to identify moments of muscle activation regardless of the individual, movement, or specific muscle. This approach aimed to simulate the real-world environment of sEMG devices.

All the presented models and methods were implemented in Python, an interpreted, general-purpose, high-level programming language. The practical operations were performed on a computer with a 3 GHz Intel Core i7 processor and 16 GB of RAM, providing the necessary computational resources for the tasks.

## 2.7. Statistical analysis

The comparison of multiple classifiers in machine learning often presents challenges, as there is no universally accepted gold standard for making such comparisons. Furthermore, many tests and studies in this field lack solid statistical foundations, leading to unjustified and

unverified conclusions. To address this issue, it is recommended to use non-parametric tests such as Wilcoxon and Friedman tests instead of parametric ones. These non-parametric tests are safer as they do not assume normal distributions or homogeneity of variances [20,37]. In this study, the Friedman's post-hoc test methodology was adopted to determine whether there is a statistically significant difference in terms of the mean values of F1-Score, Precision, and Recall among the 15 models tested with the test dataset. The test dataset consisted of the execution of three movements by four subjects, resulting in a total of 12 records.

### 3. Results

#### 3.1. Visual inspection

**Fig. 7** displays the average classification performance of different classifiers (x-axis) using different sets of features (each curve). The LGBM classifier with WAMP and NN with MIX features demonstrated the best average performance, achieving an F1-Score of  $96.52\% \pm 3.45\%$  and  $96.52\% \pm 3.07\%$ , respectively. This was followed by the NN with WAMP and XGBoost with MIX features. Notably, there were visual differences when comparing the use of only eigenvalues to WAMP or MIX features, with average F1-Scores of  $80.95\% \pm 1.64\%$ ,  $96.37\% \pm 0.067\%$ , and  $96.06\% \pm 0.52\%$ , respectively. Working solely with eigenvalues showed a lower performance compared to WAMP or MIX features. Furthermore, there was a greater standard deviation in the results when using eigenvalues compared to WAMP or MIX features. In terms of algorithm comparisons, the neural network and SVM showed similar results when using WAMP or MIX features based on the F1-Score. However, the SVM algorithm appeared to be more affected by false positive classifications (Precision Score), while demonstrating excellent performance in correctly classifying muscle activations (Recall Score). In contrast, the Extra Tree algorithm exhibited the lowest average performance with an F1-Score of  $93.71\% \pm 6.85\%$ . For more detailed information on the individual results of each subject for each algorithm and input characteristics, please refer to [Supplementary Tables S.I, S.II, and S.III](#).

Visual inspection of the classification results provides insight into the performance of the algorithms. **Fig. 8.a** displays the original signal along with a noise signal of 27. After processing, the noise signal is reduced to 3 as shown in **Fig. 8.b**, and the testing is conducted with the different models. **Fig. 8.c** and **8.d** illustrate the areas classified as muscle activation, depicted in purple, while the orange lines represent the true onset and offset of the contraction. It should be noted that the plotting is done with the original signal for visualization purposes, although the classification was performed using the noise signal. From the visual analysis, it is evident that the decision tree algorithm produces a significant number of false positives due to the introduction of noise.

A visual inspection was conducted for each of the models, similar to **Fig. 8**, to further evaluate their performance. Based on this visual inspection, it was observed that the NN + MIX, SVM + MIX, and XGBoost

+ WAMP models consistently demonstrated the best results across all test groups. [Supplementary Fig. I](#) provides a visual representation of these findings.

Regarding the windowing of the signal, the original high sampling rate of 5000 Hz (0.2 ms per sample) was reduced due to the windowing process, which encapsulates the signal information every 200 ms with a 50 % overlap. However, by knowing the positions or predicted times of muscle activity in the modified frequency, one can extrapolate and estimate the corresponding time of muscle activity in the original scale of 0.2 ms.

#### 3.2. Friedman's analysis

The analysis of variance using Friedman's test, with 15 algorithms and 12 datasets, indicated that there is no significant difference in the performance of the different machine learning algorithms evaluated in the test sets based on the F1-Score (Friedman statistic = 22.84,  $p = 0.06 > 0.05$ ). Consequently, the null hypothesis cannot be rejected. **Table 5** presents the average ranges for all models, allowing for comparisons between the models, while considering that the Friedman test verifies whether the average ranges are significantly different from each other under the null hypothesis.

Considering a significance level of 0.05, the critical value for the two-tailed Nemenyi test is 6.19, which corresponds to a critical difference (CD) of 12.32. However, as mentioned in [20], even the difference between the best and worst algorithm is smaller than the CD (ExtraTree WAMP - SVM MIX < 12.32). Therefore, the post-hoc test lacks the power to detect significant differences between the models.

To visually represent the results of the post-hoc test, a CD diagram (**Fig. 9**) can be utilized. In this diagram, groups of algorithms that are not significantly different according to the post-hoc test results are connected by a bold line. The analysis reveals that the data is insufficient to conclude whether the different algorithms have significantly different precision performance based on the F1-Score. However, significant differences are observed between the models for the Precision and Recall evaluation metrics, with p-values of 0.04 and 0.02, respectively. It is important to note that while the Friedman test indicated a significant difference ( $p < 0.05$ ), the Nemenyi test did not detect any significant difference. As mentioned in [20], this can occur due to the lower power of the post-hoc test. Thus, apart from the observation that certain algorithms differ, no further conclusions can be drawn from the results.

### 4. Discussion

The present study aimed to test and analyze different combinations of features and machine learning algorithms in order to develop a new machine learning tool for muscle activation detection.

One of the main advantages of the trained models is their statistical performance. Since there is no significant difference in the F1-Score metric, any model trained with one or all groups of features could be selected. Notably, the best average performance was obtained using the

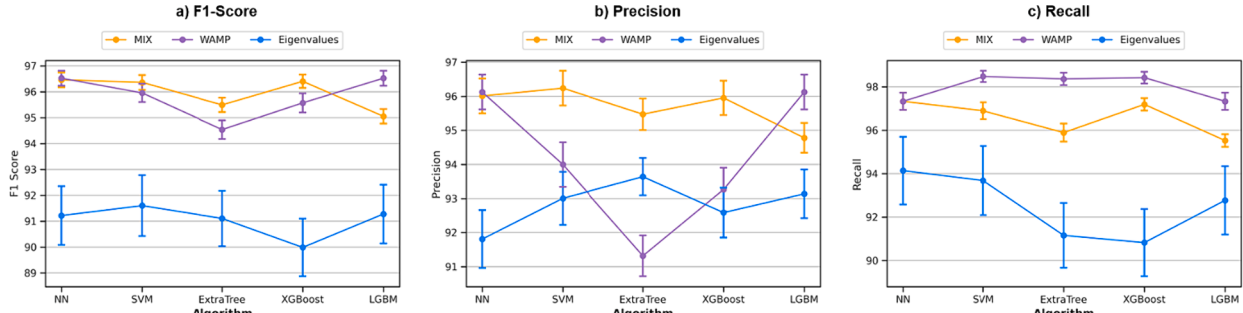


**Fig. 7.** Mean classification scores on the testing data set associated with different features.

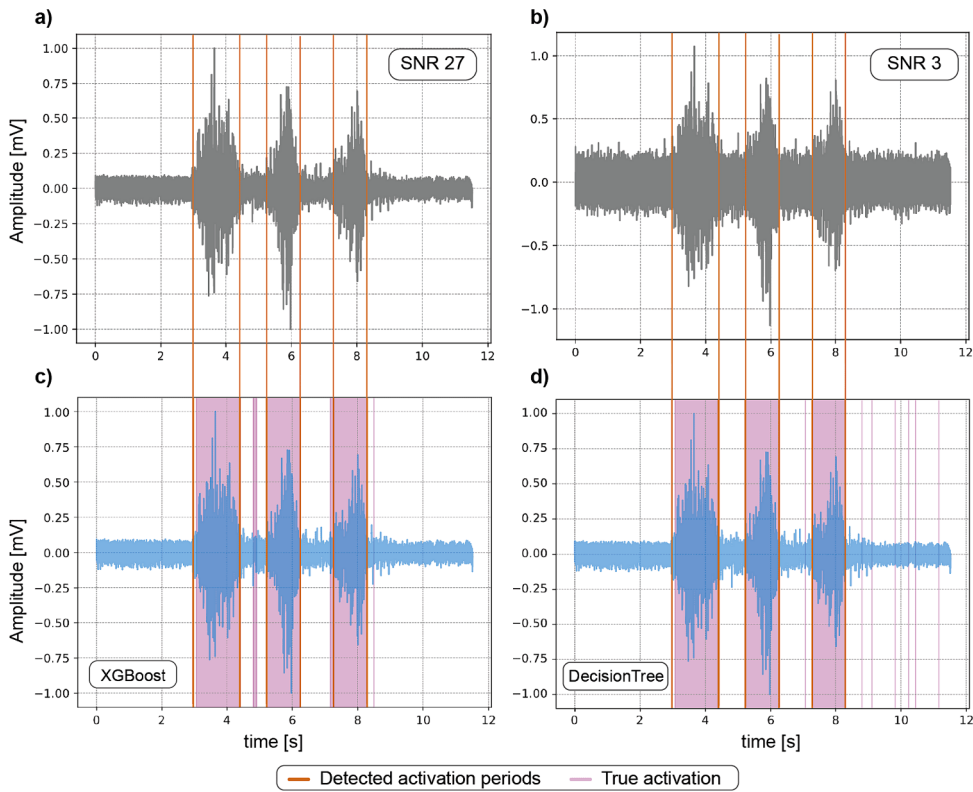


**Fig. 8.** Original signal (a) with SNR of 27 and (b) the modified signal with noise introduction SNR 3 for the movement i) of subject 1. Comparison between the predictions of the (c) XGBoost and (d) ExtraTree model for the movement i) of subject 1 with a modified SNR of 3.

**Table 5**  
Average rank for all models of Machine Learning between the test data sets from F1-Score.

| NN MIX   | SVM MIX   | ExtraTree MIX   | XGB MIX   | LGBM MIX   |
|----------|-----------|-----------------|-----------|------------|
| 6.42     | 6.04      | 8.08            | 6.67      | 8.71       |
| NN WAMP  | SVM WAMP  | ExtraTree WAMP  | XGB WAMP  | LGBM WAMP  |
| 6.12     | 7.29      | 10.54           | 8.25      | 6.12       |
| NN EIGEN | SVM EIGEN | ExtraTree EIGEN | XGB EIGEN | LGBM EIGEN |
| 8.92     | 7.75      | 9.62            | 10.62     | 8.83       |

WAMP feature. Although this feature is not commonly reported in the literature for muscle activation detection, it has shown promising results in sEMG gesture classification and real-time myoelectric activation classification, enabling the creation of human–machine interfaces [28].

In terms of wavelet decomposition, the average performance across all models was  $94.27\% \pm 2.45$ . This is slightly lower than the performance achieved by the MAEN method proposed by [40], which achieved perfect scores in terms of F1-Score, precision, and average. However, it is important to note that the signal used in the present study was intentionally distorted with noise to achieve a specific SNR of 3 dB. Lower performances were observed for lower SNR values, but when using noise signals between 16 and 30 dB, the results improved significantly, reaching scores of 97.69 %, 97.31 %, and 98.16 % for F1-Score, precision, and Recall, respectively. Notably, when using only the WAMP feature, the performance increased considerably to 99.93 %, 99.87 %, and 100 %. Further refinement of the frequency domain approach using more complex convolutional NN could provide even better results and be useful in studying neuromuscular disorders where abnormal characteristics can be identified that are imperceptible in the time domain.

The data set and experimental setup for the test group were chosen for their simplicity and reliability in detecting muscle onset and offset events during controlled movements, similar to previous studies [3,4,28,38]. However, it is worth noting that many studies evaluate their models using simulated signals [4,17,19,41]. While simulated signals offer control, they may not fully capture the truly random and stochastic nature of real signals, and the performance of models can be strongly affected when working with real data.

Additionally, the literature often focuses on controlled and simple movements, leaving room for exploration of more complex movements in sEMG signal analysis. The advantage of the APISI signal acquisition and processing platform lies in its ability to train models with signals from different individuals and muscles, preventing potential overfitting and allowing for analysis of complex signals. These models, given their promising statistical performance, could find utility in real-time applications such as assistive technologies, prosthetics, or rehabilitation devices [6,11,18,39]. Considering their computing requirements, the efficient processing of real-time data necessitates a careful evaluation of computational resources and algorithmic efficiency. Moreover, the applicability of these models for specific use cases, such as continuous monitoring of muscle activity in clinical settings or real-time feedback in rehabilitation exercises, underscores their potential impact on enhancing human–machine interactions and healthcare outcomes.

The proposed approach has successfully enabled the evaluation of 15 models for detecting muscle activity from real sEMG records under various noise conditions, emphasizing a promising approach by incorporating the underexplored WAMP feature and their combination with DWT. This is an aspect that has not been extensively explored in the context of Machine Learning and EMGs until now.

Finally, although all the models achieved an average performance of 94.73 %, it is important to consider the computational time required for signal processing before inputting data into the machine learning algorithm. Real-time implementation of these models should be carefully evaluated. For example, the DEMANN approach proposed by [4], where

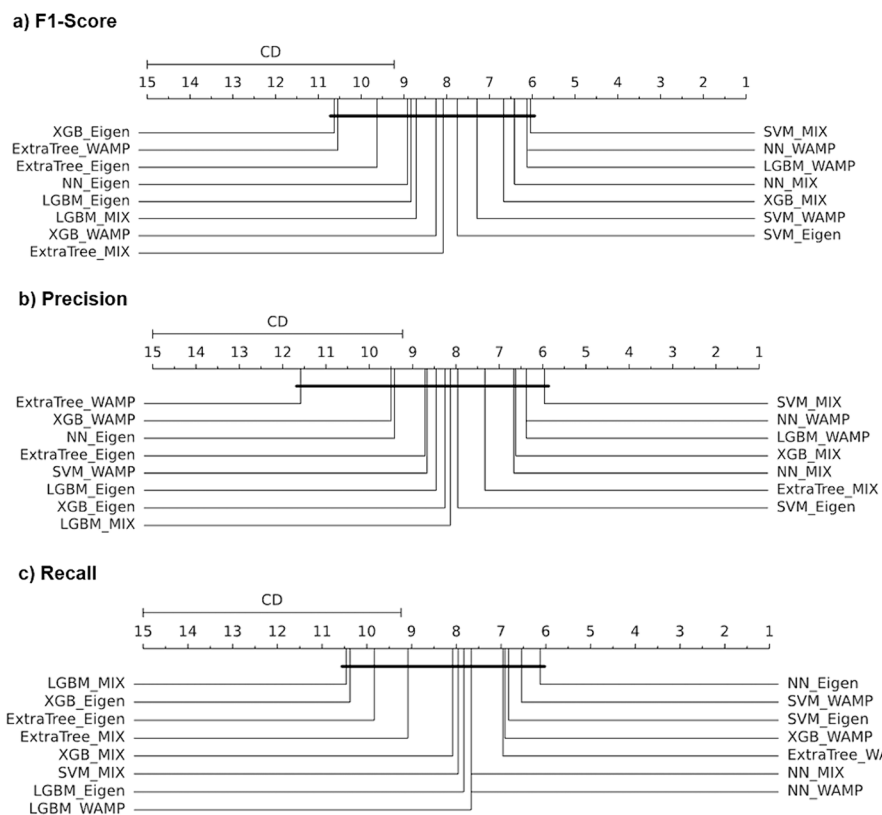


**Fig. 9.** Comparison of all the classifiers with each other with the Nemenyi test with  $p = 0.05$ , for the evaluation of metrics (a) F1 Score, (b) Precision, (c) Recall.

**Table 6**  
Summary of machine learning methods using in sEMG signal activation.

| Author             | Year | Subjects  | Parts  | Method                                    | Results   | Reference |
|--------------------|------|---|--|---|---|-----------|
| Francesco Di Nardo | 2022 | 1) 720 simulated sEMG signal<br>2) 18 adult subjects<br>3) Obese and overweight volunteers (BMI > 25) and subjects affected by any pathological condition | 1) –<br>2) Upper and lower limb<br>3) Lower limb   | Continuous wavelets transform (CWT)       | Mean absolute error simulated and real datasets of ≈10 ms and <30 ms respectively   | [40]      |
| Francesco Di Nardo | 2022 | 1) Simulated sEMG signal varying SNR from 1 to 30 dB<br>2) 18 participants performing knee extension and elbow flexion.<br>3) 30 healthy adults           | 1) -<br>2) Vastus lateralis, biceps brachii<br>3) Gastrocnemius lateralis, tibialis anterior, and vastus lateralis | DEMANN                                    | Mean accuracy ( $\pm$ SD) of $97.8 \pm 3.0\%$   | [4]       |
| Marco Ghislieri    | 2021 | 1) Simulated sEMG signals<br>2) 8 healthy individuals, and 12 patients affected by neurological or orthopedic pathologies                                 | 1) -<br>2) Lower limb  | LSTM                                      | Overall classification accuracy of 97 % (simulated data) and 90 % (real data)   | [17]      |
| Y. Jiang           | 2020 | 15 healthy subjects   | 12 upper limb muscles  | CNN                                       | Average accuracy for motion pattern recognition ranged from 69.96 to 97.5 %   | [42]      |
| Ali Raza Asif      | 2020 | 18 healthy male subjects  | Upper limb and wrist   | CNN                                       | sEMG pattern recognition activation close hand, flex hand, extend the hand and fine grip): $83.7\% \pm 13.5\%$ , $71.2\% \pm 20.2\%$ , $82.6\% \pm 13.9\%$ and $74.6\% \pm 15\%$ , respectively | [43]      |
| Iman Akef Khawaled | 2019 | Simulated sEMG signals  | –  | Neural muscle activation detection (NMAD) | Absolute latency less than 5 ms for signals between 1 and 8 dB  | [19]      |
| Giuseppe Vannozzi  | 2010 | 1) Simulated sEMG signals<br>2) Ten able-bodied male subjects   | Lower limb   | Wavelet transform detection algorithm     | Low percentages of false positives (less than 7 %) and absence of missed detection were found   | [41]      |
| Xiaoyan Li         | 2005 | Four healthy subjects   | Lower limb   | TKEO                                      | Latency time in worst and best case of $28.76 \pm 30.59$ , $19.06 \pm 24.78$ ms respectively for 2, 10 dB (SNR)   | [3]       |

onset/offset events are predicted in subsequent 10 ms windows, can be a suitable tool for real-time applications.

#### 4.1. The state-of-the-arts of sEMG signal activation algorithms

Various strategies have expanded research into applications of machine learning algorithms for pattern recognition in sEMG signals (Table 6) exploring features in both the time and frequency domains, addressing different muscles, types of contraction, and movement patterns. This opens the possibility for substantial improvements in recognition processes. Notable methods include the Wavelet Transform (WT) [40,41] for detecting activation intervals, amplitude threshold-based strategies like TKEO [3], and neural networks such as CNN, achieving accuracies ranging from 69.96 % to 97.5 % [42,43]. The Long Short-Term Memory (LSTM) method [17], designed for temporal patterns, has achieved an accuracy of up to 90 % in real data. Simulated signal-based methods, like NMAD [19] and DEMANN [4], have also been explored, reaching accuracies of up to 97.8 %. The accuracy in pattern recognition varies significantly among studies, with results ranging from approximately 70 % to over 97 %. This suggests that the choice of processing method and specific application has a crucial impact on performance. Studies address various applications, from knee extension and elbow flexion to more specific actions such as hand closure, hand flexion, and extension. This indicates the adaptability of sEMG techniques for different contexts and clinical applications.

Most of these studies involved between 10 and 30 volunteers, and some incorporated effects with different signal-to-noise ratios (SNR) to replicate conditions closer to reality. While machine learning methods prove to be accurate and robust in recognizing motion patterns based on sEMG, the challenge remains in achieving short processing times and maintaining high accuracies for their effective implementation in robotics and prosthetics applications.

## 5. Conclusions

While the Friedman test revealed a significant difference in the Recall and Precision metrics, it is important to note that the F1-Score combines both Precision and Recall into a single value. In the case of muscle activation detection, the goal is to minimize false positives while detecting the maximum number of muscle activations. Therefore, the F1-Score is the appropriate metric for evaluating the models and provides a better overall assessment of their performance.

Among the five tested algorithms, the ExtraTree algorithm showed more difficulty in avoiding false positives, while NN and SVM performed better. Although there is no significant difference between the models, visual inspection revealed that the NN, SVM, and XGBoost models achieved the best performance when using the MIX features for the first two algorithms and the WAMP feature for XGBoost. Additionally, most models exhibited false positives with durations ranging from 0.1 to 0.2 s. To address this, post-processing or cleaning of the results could be implemented, ignoring activations lasting less than 0.2 s to obtain more accurate estimates.

Due to the stochastic nature of the underlying signal, objective error measures are not applicable for determining the start and stop times of muscle activation. Instead, the automatically determined onsets were compared to results obtained through visual inspection by a trained sEMG examiner.

One of the key advantages of machine learning models is their ability to extract relationships between different features and output values. Therefore, a crucial task is to identify the best features that optimize the models. For future research, it would be interesting to explore different parameters such as signal window size, number of wavelet decompositions, and feature selection techniques to find the most informative features for the models. Additionally, the implementation of unsupervised deep learning approaches is another area to be explored, as it could potentially improve performance by eliminating the need for

manual labeling to train the models.

The proposed approach in this research has shown promising results in automatically detecting sEMG records associated with slow and controlled movements in healthy individuals. However, it has not been tested with fast and explosive movements commonly found in certain high-speed sports, as well as in records from individuals with musculoskeletal pathologies. The limitation of this study opens avenues for future research, emphasizing the need to assess the development in the context of rapid sEMG dynamics and those occurring under conditions of illness.

## CRediT authorship contribution statement

**Valentina Mejía Gallón:** Writing – review & editing, Writing – original draft, Visualization, Software, Methodology, Investigation, Formal analysis. **Stirley Madrid Vélez:** Writing – review & editing, Visualization, Validation, Software, Methodology, Investigation. **Juan Ramírez:** Writing – review & editing, Supervision, Project administration. **Freddy Bolaños:** Validation, Supervision.

## Declaration of competing interest

The authors declare that they have no known competing financial interests or personal relationships that could have appeared to influence the work reported in this paper.

## Data availability

Data will be made available on request.

## Acknowledgments

Authors would like to thank the Universidad Nacional de Colombia for the support received around this research.

## Appendix A. Supplementary material

Supplementary data to this article can be found online at <https://doi.org/10.1016/j.bpsc.2024.106266>.

## References

- [1] C. Seyidbayli, F. Salhi, E. Akdogan, Comparison of machine learning algorithms for EMG signal classification, Period. Eng., Nat. Sci. 8 (2) (2020) 1165–1176, <https://doi.org/10.21533/pen.v8i2.1293>.
- [2] S. Solnik, P. Rider, K. Steinweg, P. DeVita, T. Hortobágyi, Teager–Kaiser energy operator signal conditioning improves EMG onset detection, Eur. J. Appl. Physiol. 110 (3) (2010) 489–498, <https://doi.org/10.1007/s00421-010-1521-8>.
- [3] X. Li, A.S. Aruin, Muscle activity onset time detection using Teager–Kaiser energy operator, in: Conf. Proc. IEEE Eng. Med. Biol. Soc. 27th Annual Conference, Vol. 2005, IEEE, 2005, pp. 7549–7552, doi: 10.1109/IEMBS.2005.1616259.
- [4] F. Di Nardo, A. Nocera, A. Cucchiarelli, S. Fioretti, C. Morbidoni, Machine learning for detection of muscular activity from surface EMG signals, Sensors (Basel) 22 (9) (2022) 3393, <https://doi.org/10.3390/s22093393>.
- [5] R.H. Chowdhury, M.B.I. Reaz, M.A. Ali, A.A. Bakar, K. Chellappan, T.G. Chang, Surface electromyography signal processing and classification techniques, Sensors (Basel) 13 (9) (2013) 12431–12466, <https://doi.org/10.3390/s130912431>.
- [6] M.U. Khan, Z.A. Choudry, S. Aziz, S.Z.H. Naqvi, A. Aymin, M.A. Intiaz, Biometric authentication based on EMG signals of Speech, in: 2020 in International Conference on Electrical, Communication, and Computer Engineering (ICECCE), IEEE, Jun. 2020, pp. 1–5, doi: 10.1109/ICECCE49384.2020.9179354.
- [7] A. Subasi, M.K. Kiyimli, Muscle fatigue detection in EMG using time-frequency methods, ICA and neural networks, J. Med. Syst. 34 (4) (2010) 777–785, <https://doi.org/10.1007/s10916-009-9292-7>.
- [8] P.A. Karthick, D.M. Ghosh, S. Ramakrishnan, Surface electromyography based muscle fatigue detection using high-resolution time-frequency methods and machine learning algorithms, Comput. Methods Programs Biomed. 154 (2018) 45–56, <https://doi.org/10.1016/J.CMPB.2017.10.024>.
- [9] M.R. Ahsan, M.I. Ibrahimy, O.O. Khalifa, EMG signal classification for human computer interaction: a review, Eur. J. Sci. Res. 33(3) (2009) 480–501, Available: <http://www.eurojournals.com/ejsr.htm>.

- [10] J. Tryon, E. Friedman, A.L. Trejos, Performance evaluation of EEG/EMG fusion methods for motion classification, *IEEE Int. Conf. Rehabil. Robot.* 2019 (2019) 971–976, <https://doi.org/10.1109/ICORR.2019.8779465>.
- [11] A. Subasi, M. Yilmaz, H.R. Ozcalik, Classification of EMG signals using wavelet neural network, *J. Neurosci. Methods* 156 (1–2) (2006) 360–367, <https://doi.org/10.1016/J.JNEUMETH.2006.03.004>.
- [12] C.S. Pattichis, C.N. Schizas, L.T. Middleton, Neural network models in EMG diagnosis, *IEEE Trans. Biomed. Eng.* 42 (5) (1995) 486–496, <https://doi.org/10.1109/10.376153>.
- [13] R. Martinek, et al., Advanced bioelectrical signal processing methods: past, present and future approach—Part I: cardiac signals, *Sensors (Basel)* 21 (15) (2021) 5186, <https://doi.org/10.3390/S21155186>.
- [14] A. Alkan, M. Günay, Identification of EMG signals using discriminant analysis and SVM classifier, *Expert Syst. Appl.* 39 (1) (2012) 44–47, <https://doi.org/10.1016/J.ESWA.2011.06.043>.
- [15] A. Subasi, Classification of EMG signals using PSO optimized SVM for diagnosis of neuromuscular disorders, *Comput. Biol. Med.* 43 (5) (2013) 576–586, <https://doi.org/10.1016/J.COMPBIOMED.2013.01.020>.
- [16] A. Hiraiwa, K. Shimohara, Y. Tokunaga, EMG pattern analysis and classification by neural network, in: Proceedings of the IEEE Int. Conf. Syst. Man Cybern., Vol. 3, 1989, pp. 1113–1115, doi: 10.1109/ICSMC.1989.71472.
- [17] M. Ghislieri, G.L. Cerone, M. Knaflitz, V. Agostini, Long short-term memory (LSTM) recurrent neural network for muscle activity detection, *J. Neuroeng. Rehabil.* 18 (1) (2021) 153, <https://doi.org/10.1186/S12984-021-00945-W/FIGURES/6>.
- [18] U. Rashid, I.K. Niazi, N. Signal, D. Farina, D. Taylor, Optimal automatic detection of muscle activation intervals, *J. Electromyogr. Kinesiol.* 48 (2019) 103–111, <https://doi.org/10.1016/J.JELEKIN.2019.06.010>.
- [19] I. Akef Khawaled, A. Abotabl, Neural muscle activation detection: a deep learning approach using surface electromyography, *J. Biomech.* 95 (2019) 109322, <https://doi.org/10.1016/j.jbiomech.2019.109322>.
- [20] J. Demsar, Statistical comparisons of Classifiers over multiple data sets, *J. Mach. Learn. Res.* 7 (2006) 1–30 [Online], Available: <http://arxiv.org/abs/1810.04805>.
- [21] P. Nemenyi, Distribution-free multiple comparisons, 1963 [Online], Available: <https://www.worldcat.org/es/title/distribution-free-multiple-comparisons/oclc/39810544> Princeton University.
- [22] J.G. Webster, A.J. Nimunkar, J.W. Clark, Medical instrumentation: application and design, fourth edition, 2010.
- [23] F. Hug, Can muscle coordination be precisely studied by surface electromyography? *J. Electromyogr. Kinesiol.* 21 (1) (2011) 1–12, <https://doi.org/10.1016/J.JELEKIN.2010.08.009>.
- [24] J. Liu, D. Ying, P. Zhou, Wiener filtering of surface EMG with a priori SNR estimation toward myoelectric control for neurological injury patients, *Med. Eng. Phys.* 36 (12) (2014) 1711–1715, <https://doi.org/10.1016/J.MEDENGPHY.2014.09.008>.
- [25] S. Karheily, A. Moukadem, J.-B. Courbot, D. Abdeslam, Time-frequency features for sEMG signals classification, in: Proceedings of the 13th international joint conference on biomedical engineering systems and technologies, SCITEPRESS – Science and Technology Publications, 2020, pp. 244–249, doi: 10.5220/0008971902440249.
- [26] A. Phinyomark, C. Limsakul, P. Phukpattaranont, EMG feature extraction for tolerance of white Gaussian noise, *Work. Symp. Sci. Technol.*, 2008.
- [27] N. Malešević, D. Marković, G. Kanitz, M. Controzzi, C. Cipriani, C. Antfolk, Vector autoregressive hierarchical hidden Markov models for extracting finger movements using multichannel surface EMG signals, *Complexity* 2018 (2018) 1–12, <https://doi.org/10.1155/2018/9728264>.
- [28] A. Turner, D. Shieff, A. Dwivedi, M. Liarokapis, Comparing machine learning methods and feature extraction techniques for the EMG based decoding of human intention, in: *Annu. Int. Conf. IEEE Eng. Med. Biol. Soc. 43rd Annual International Conference of the IEEE Engineering in Medicine & Biology Society (EMBC)*, vol. 2021, Nov. 2021, IEEE, 2021, pp. 4738–4743, doi: 10.1109/EMBC46164.2021.9630998.
- [29] S. Lahmiri, Wavelet low- and high-frequency components as features for predicting stock prices with backpropagation neural networks, *J. King Saud Univ. Comput. Inf. Sci.* 26 (2) (2014) 218–227, <https://doi.org/10.1016/j.jksuci.2013.12.001>.
- [30] F. Duan, L. Dai, W. Chang, Z. Chen, C. Zhu, W. Li, sEMG-based identification of hand motion commands using wavelet neural network combined with discrete wavelet transform, *IEEE Trans. Ind. Electron.* 63 (3) (2016) 1923–1934, <https://doi.org/10.1109/TIE.2015.2497212>.
- [31] J. Kilby, H.G. Gholam Hosseini, Wavelet analysis of surface electromyography signals, in: *Conf. Proc. IEEE Eng. Med. Biol. Soc. The 26th Annual International Conference of the IEEE Engineering in Medicine and Biology Society*, vol. 2006, IEEE, 2004, pp. 384–387, doi: 10.1109/EMBS.2004.1403174.
- [32] J. Kilby, G. Mawston, H.G. Hosseini, Analysis of surface electromyography signals using continuous wavelet transform for feature extraction, in: *2006 IET Conf. Publ.*, no. 520, pp. 23, doi: 10.1049/CP:20060353.
- [33] N.S. Rekhi, H. Singh, A.S. Arora, A.K. Rekhi, Analysis of EMG signal using wavelet coefficients for upper limb function, in: *2009 2nd IEEE International Conference on Computer Science and Information Technology*, vol. 2009, IEEE, pp. 357–361, doi: 10.1109/ICCSIT.2009.5234929.
- [34] T. Chen, C. Guestrin, XGBoost: a scalable tree boosting system, 2016, doi: 10.1145/2939672.2939785.
- [35] G. Ke et al., LightGBM: a highly efficient gradient boosting decision tree [Online], Available: <https://github.com/Microsoft/LightGBM>.
- [36] L. Yang, A. Shami, On hyperparameter optimization of machine learning algorithms: theory and practice, *Neurocomputing* 415 (2020) 295–316, <https://doi.org/10.1016/J.NEUCOM.2020.07.061>.
- [37] R. Ghorbani, R. Ghousi, Comparing different resampling methods in predicting students' performance using machine learning techniques, *IEEE Access* 8 (2020) 67899–67911, <https://doi.org/10.1109/ACCESS.2020.2986809>.
- [38] G. Rescio, A. Leone, P. Siciliano, Supervised machine learning scheme for electromyography-based pre-fall detection system, *Expert Syst. Appl.* 100 (2018) 95–105, <https://doi.org/10.1016/j.eswa.2018.01.047>.
- [39] M. Yu, G. Li, D. Jiang, G. Jiang, B. Tao, D. Chen, Hand medical monitoring system based on machine learning and optimal EMG feature set, *Pers. Ubiquit. Comput.* (2019), <https://doi.org/10.1007/s00779-019-01285-z>.
- [40] F. Di Nardo, T. Basili, S. Meletani, D. Scaradozzi, Wavelet-based assessment of the muscle-activation frequency range by EMG analysis, *IEEE Access* 10 (2022) 9793–9805, <https://doi.org/10.1109/ACCESS.2022.3141162>.
- [41] G. Vannozzi, S. Conforto, T. D'Alessio, Automatic detection of surface EMG activation timing using a wavelet transform based method, *J. Electromogr. Kinesiol.* 20 (4) (2010) 767–772, <https://doi.org/10.1016/j.jeletekin.2010.02.007>.
- [42] Y. Jiang, C. Chen, X. Zhang, C. Chen, Y. Zhou, G. Ni, S. Muñ, S. Lemos, Shoulder muscle activation pattern recognition based on sEMG and machine learning algorithms, *Comput. Methods Progr. Biomed.* 197 (2020) 105721, <https://doi.org/10.1016/j.cmpb.2020.105721>.
- [43] A.R. Asif, A. Waris, S.O. Gilani, M. Jamil, H. Ashraf, M. Shafique, I.K. Niazi, Performance evaluation of convolutional neural network for hand gesture recognition using EMG, *Sensors (Basel)* 20 (6) (2020) 1642, <https://doi.org/10.3390/s20061642>.